NUMERICAL MODELLING OF CORNER POINT SINGULARITIES AND THEIR EFFECT ON THE CLOSURE BEHAVIOUR OF 3D FATIGUE CRACKS

P. F. P. de Matos[1] and D. Nowell[2]

[1]Instituto Superior de Entre Douro e Vouga, Rua António de Castro Corte Real,
4520-909 Santa Maria da Feira, Portugal.
E-mail: pfpmatos@engenheiros.pt

[2]University of Oxford, Department of Engineering Science, Parks Road, Oxford,
OX1 3PJ, United Kingdom.
david.nowell@eng.ox.ac.uk

ABSTRACT

Although real cracks are inherently three-dimensional, relatively little effort has been put into the study of 3D cracks from both linear elastic and elastic-plastic points of view. Analytical solutions are difficult to obtain, and three-dimensional numerical simulations are complex and time consuming. Due to these limitations, the understanding of three-dimensional fatigue crack propagation has remained a challenging problem for the fatigue research community. The need to improve fatigue life predictions, particularly in aircraft structures, has been a motivation for research in this area. One of the outcomes of the research carried out over the last few decades is that fatigue cracks in metals are partially closed over part of the load cycle. This phenomenon of crack closure is thought by many to be the key to understanding the effect of non-uniform loading.This paper investigates the influence of surface effects on the closure behaviour of 3D fatigue cracks. Linear elastic analyses of 3D cracks show that Poisson's ratio influences the stress field close to the free surface. A 'corner point' singularity exists which differs from the usual $1/\sqrt{r}$ value for 2D cracks. In this region, both crack closure and corner point singularities are essentially "free surface" effects and it is difficult to investigate 3D crack closure without addressing the associated stress singularity problem. The aim of this paper is to investigate the influence of free surface effects on the closure behavior of 3D fatigue cracks, addressing some numerical difficulties related to FE modeling of the problem.

KEY WORDS: 3D cracks; Corner point singularity; Free surface; Crack closure.

1. INTRODUCTION

One of the difficulties in modelling 3D cracks is related to the shape of the crack front, which is often assumed to intersect the free surface at 90º. Under these conditions, the order of the stress singularity may differ from the usual square root singular K-field. In such 3D crack problems the order of the singularity at the free surface depends on Poisson's ratio and the intersection angle of the crack front with the free surface [1,2,3,4]. It seems reasonable to suggest that, real mode I fatigue cracks might choose to preserve the $1/\sqrt{r}$ singularity and therefore the crack front tends to intersect the free surface at a critical angle ($\beta_c \neq 0^o$) which is a function of the Poisson's ratio of the material and ensures square-root singularity.

In a recent paper, Heyder *et al.* [1] report experimental measurements of the angle at which crack fronts break the free surface for transparent specimens (PMMA) under four-point bending. They have shown that, at least for mode I crack propagation, the crack front is shaped so as to ensure square-root singularity at the intersection of the crack front with the free surface. Therefore, in real materials ($\nu \neq 0$) the assumption, frequently made in models, that the crack front intersects the free surface at 90º will modify the order of singularity of the stress field in the region of the crack front close to the free surface. This may complicate the interpretation of crack closure in this region, and is important, since it is in the surface layer where closure effect are likely to be most significant [5,6,7]; incorrect modelling of the stress state will present difficulties when comparing modelling to experimental data. Since both phenomena, corner point singularities and crack closure, may co-exist and have a significant effect close to the free surface, we have divided our work in two parts. In the first part, we examine a 3D linear elastic crack and modify the shape of the crack front, for different values of Poisson's ratio, in order to ensure square-root singularity at the corner point (see Figure 1). In the second part of the paper, an elasto-plastic growing crack is modelled in a finite plate. The closure behaviour is studied for different values of Poisson's ratio for both, straight and modified crack fronts. Finally, based on the results obtained, some conclusions are drawn.

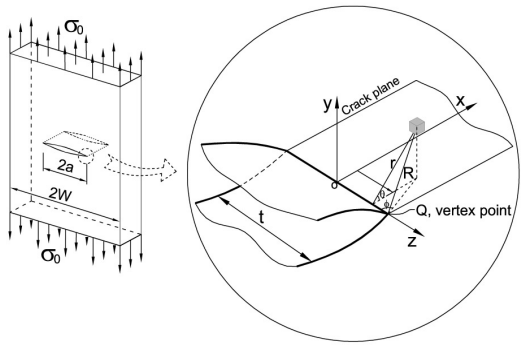

Figure 1. Rectangular plate with a central straight through crack. Coordinate system for a point in the vicinity of the crack front.

2. SINGULARITIES IN 3D CRACKED BODIES

Shivakumar and Raju [4] showd that two different types of stress singularities co-exist along the crack front of 3D cracks, such as in the problem to be analysed (Fig. 1.). One is the conventional cylindrical singularity, and the second is the vertex singularity, which is assumed to exist at the corner point (point Q in Figure 1).

2.1. Cylindrical singularity

The stress and displacement fields of the cylindrical singularity can be expressed as,

$$\sigma_{ij} = C_{ij}(\theta, z) \cdot r^{\lambda_\sigma} \quad (1)$$

$$u_{ij} = D_{ij}(\theta, z) \cdot r^{\lambda_u} \quad (2)$$

where $C_{i,j}$ and $D_{i,j}$ are functions of z and θ. Both λ_σ, λ_u are independent of spatial coordinates r, θ and z and $\lambda_\sigma = \lambda_u - 1$.

2.2. Vertex singularity

Benthem [2, 3] used the vertex type of singularity to describe the singular stress field at the intersection of crack front and free surface (point Q in Figure 1). The stress and displacement field equation for this type of singularity can be written as follows,

$$\sigma_{ij} = E_{ij}(\theta, \phi) \cdot R^{\lambda_\sigma} \quad (3)$$

$$u_{ij} = F_{ij}(\theta, \phi) \cdot R^{\lambda_u} \quad (4)$$

where the functions E_{ij} and F_{ij} are functions of θ and ϕ, and R is the distance between the corner point and the point at which the stress is evaluated. In this case λ_σ, λ_u are functions of the Poisson's ratio and, once again, $\lambda_\sigma = \lambda_u - 1$.

2.3. Cylindrical and Vertex singularities

Based on a superposition argument, Shivakumar and Raju [4] suggested that the stress field of a 3D plate under remote tension can be written as the superposition of the stress field from a plane strain plate under remote tension together with corrective tractions on the free surface of the 3D plate. Hence they concluded that the stress and displacement fields can be expressed as follows,

$$\sigma_{ij} = C_{ij}(\theta, z) \cdot r^{-1/2} + E'_{ij} \cdot R^{\lambda_\sigma} \quad (5)$$

$$u_{ij} = D_{ij}(\theta, z) \cdot r^{-1/2} + F'_{ij} \cdot R^{\lambda_u} \quad (6)$$

In these equations the first term is the conventional cylindrical singularity associated with the stress intensity factor, which is dominant along most of the crack front. The second term is either a vertex or cylindrical singularity. Shivakumar and Raju [4] obtained good agreement between their FE solution and Benthem's [2, 3] solution for a vertex singularity. The relative influence of each of these singularities depends on the value of Poisson's ratio.

3. SINGULARITIES IN 3D CRACKED BODIES

This section presents details of the finite element analysis performed to quantify the order of stress singularity along the crack front, using a log–log type of regression analysis. The case where the crack front is normal to the free surface was studied for different values of Poisson's ratio (ν = 0, 0.1, 0.2, 0.3, 0.4 and 0.45). The material is assumed to be isotropic with positive Poisson's ratio. After identifying the region where the classical square-root singularity is not the dominant term, the shape of the crack front was modified for specific values of the Poisson's ratio (ν= 0.2, 0.3 and 0.4), in order to ensure square-root behaviour at the corner point.

3.1. Linear elastic FE modelling

The geometry of the problem under study is presented in Figure 2. It consists of a square plate with a finite central crack. For convenience only one eighth of the plate was modelled. The dimensions of the plate are W = 100 mm with a central crack a_0 = 10 mm, and thickness t of 10 mm. For a linear elastic analysis the material behaviour is defined by Young's Modulus (E) and Poisson's ratio. In the present work E = 100 GPa and Poisson's ratio ν = 0, 0.1, 0.2, 0.3, 0.4 and 0.45.

Figure 3 shows the finite element mesh used. This mesh has 106160 isoparametric brick elements (C3D20), each with twenty nodes, and was designed with an increasing level of refinement towards the crack front region. The level of mesh refinement was set by reference to a convergence analysis carried out in 2D plane strain. The element size for the 3D analysis corresponded to that for the highest refinement level in 2D. Twenty layers of elements were used through the thickness of the plate with decreasing thickness from the centre of the plate towards the free surface (see Figure 3b). The thickness of the layers at the center of the plate and at the free surface is 0.469 mm and 0.031 mm, respectively.

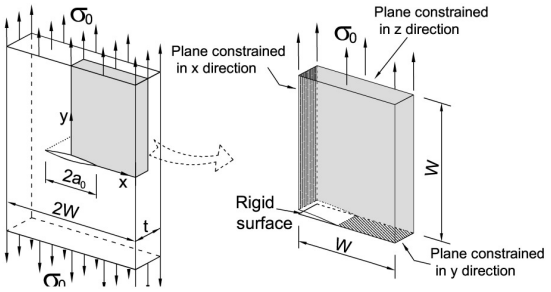

Figure 2. Rectangular plate with a central straight through crack, geometry and boundary conditions.

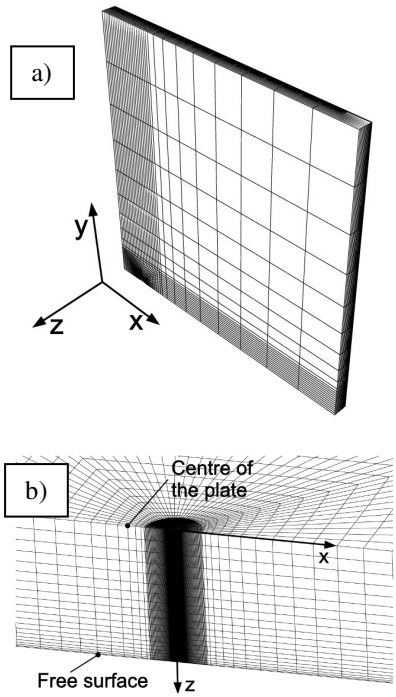

Figure 3. Mesh details, 3D model: (a) Mesh of a square plate with 100 x 100 mm with an initial crack (a_0) of 10 mm and thickness (t) of 10 mm; (b) Mesh detail of the crack front, crack front lies along z axis.

3.2. Log–log regression analysis

The log–log regression analysis is based on the nodal stresses and displacements from the finite element analysis (FEA). A Matlab routine was written to read the nodal coordinates, nodal stresses and displacements from the FEA at different inclinations h for different r values and different coordinates z. For each inclination θ, an analysis along the crack front was performed for 41 rows with different z coordinates shown schematically in the following figure.

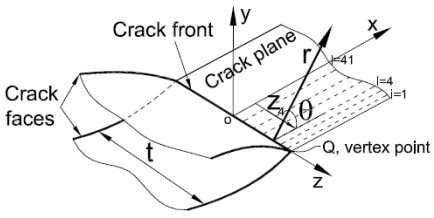

Figure 4. 3D crack front, coordinate systems.

The analysis was carried out for five different θ values (θ= 0º, 45º, 90º, 135º and 180º). It will be apparent that σ_y is zero along the crack faces (h = 180º) and u_y = 0 along the plane ahead of the crack tip (θ = 0º). Hence, for θ≤ 90º the regression analysis was performed based on the stresses on the y direction (σ_y), for θ = 135º and 180º displacements on the y direction (u_y) were used. Given the difficulty of evaluating two coefficients and one exponent in equations (5) and (6), these equations were simplified to one constant and one exponent as suggested in [4]

$$\sigma_y = C \cdot r^{\lambda_\sigma} \tag{7}$$

$$u_y = D \cdot r^{\lambda_u} \tag{8}$$

Taking logarithms on both sides of equations (7) and (8) we obtain the following two equations

$$\log(\sigma_y) = \log(C) + \lambda_\sigma \cdot \log(r) \tag{7}$$

$$\log(u_y) = \log(D) + \lambda_u \cdot \log(r) \tag{8}$$

λ_σ and λ_u may now be calculated based on the best fit of a straight line to the plot of log(σ_y or u_y) vs. log(r). As an example Figure 5 shows the stresses and displacements for different z/t coordinates for θ = 0º and 180º, respectively.

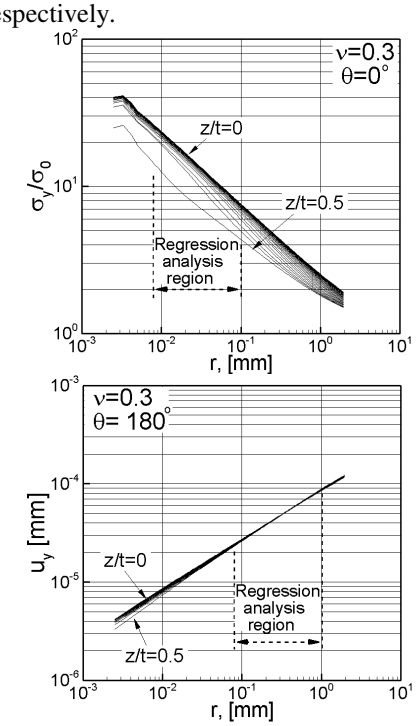

Figure 5. Log-log regression analysis region: a) Stresses for different z/t coordinates and θ=0º; b) Displacements u_y for different z/t coordinates and θ=180º.

The lower and upper limits for the regression analysis were chosen taking into account that values very close to the crack tip will be inaccurate due to an inability of the FE shape functions to model displacements accurately; and values further away from the crack tip will include higher order terms. The upper limit was selected taking into account the region close to the crack tip where classical the stress intensity factor governs the stress field, r/a ≈ 0.1 is usually taken as a reference.

3.3 Power of the stress singularity and displacement and thickness of the boundary layer

Using the regression analysis described above it was possible to estimate the power of the dominant stress singularity (λ_σ) and displacement (λ_u) along the crack front. This analysis was performed for a range of Poisson's ratio values as shown in Figure 6.

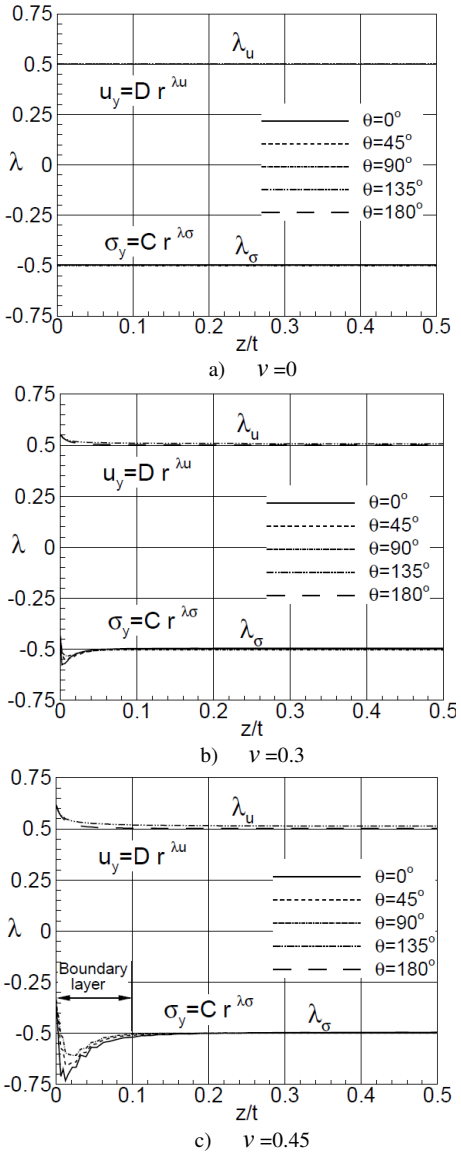

Figure 6. Log- Power of the stress singularity and displacement along the crack front for ν =0, 0.3 and 0.45.

It can be clearly seen that, independently of the value of Poisson's ratio and of the plane of analysis, θ, the power of the stress singularity at the centre of the plate (z/t = 0) is 0.5. In addition, the variables separable assumption is valid on this region since ($\lambda_\sigma = \lambda_u - 1$). For the case ν =0, the power of the stress singularity along the crack front is constant and square-root singular without showing any influence of the free surface, this is expected since β_c = 0º for ν = 0. For larger values of Poisson's ratio the stress singularity is weaker at the free surface (z/t=0.5). Some specific results are shown in Table 1, which can be compared with results available in the literature shown in Table 2.

Table 1 - Power of the stress and displacement at mid-plane and free surface for different values of the Poisson's ratio

Poisson's ratio (ν)	Present work – free surface ($z/t = 0.5$)				
	λ_σ ($\theta = 0°$)	λ_σ ($\theta = 45°$)	λ_σ ($\theta = 90°$)	$\lambda_u - 1$ ($\theta = 135°$)	$\lambda_u - 1$ ($\theta = 180°$)
0.00	−0.495	−0.496	−0.501	−0.499	−0.499
0.10	−0.489	−0.485	−0.492	−0.488	−0.489
0.20	−0.477	−0.467	−0.475	−0.473	−0.474
0.30	−0.452	−0.434	−0.447	−0.449	−0.451
0.40	−0.395	−0.401	−0.408	−0.413	−0.412
0.45	−0.354	−0.334	−0.374	−0.386	−0.382
0.49	–	–	–	−0.359	−0.354
0.50	–	–	–	−0.341	−0.333
	Present work – mid-plane ($z/t = 0$)				
0.00	−0.495	−0.496	−0.501	−0.499	−0.499
0.10	−0.495	−0.496	−0.503	−0.497	−0.499
0.20	−0.494	−0.496	−0.504	−0.495	−0.499
0.30	−0.494	−0.497	−0.503	−0.507	−0.498
0.40	−0.496	−0.498	−0.501	−0.489	−0.499
0.45	−0.494	−0.496	−0.499	−0.487	−0.498
0.49	−0.491	−0.496	−0.499	−0.483	−0.498
0.50	–	–	–	−0.485	−0.496

Table 2 - Reference values for the power of the stress singularity and displacement for different values of the Poisson's ratio at the free surface

Poisson's ratio, v	Benthen [2,3]	Shivakumar and Raju [4]		Bažant and Estenssoro [8]
	λ_σ	λ_σ (θ=0º)	λ_u -1 (θ=180º)	λ_σ
0,00	-0,5	-0,497	-0,497	---
0,30	-0,452	-0,451	-0,452	-0,452
0,40	-0,414	-0,407	-0,417	-0,413
0,45	---	-0,356	-0,391	---
0,50	-0,332	---	---	---

It can be seen that the present results are in good agreement with those from references [2,3,4,8].
The region close to the free surface where the stresses are not square-root singular (e.g. Figures 6 b and c) is usually called the boundary layer region. In interpreting the results the thickness of the boundary layer was calculated using the first point along the crack front where the stress singularity exceeds 1% of the order of the stress singularity at the centre of the plate (see Figure 6 c). Using this criteria the thickness of the boundary layer is 0%, 1%, 2.5%, 4%, 12.5% and 15 % of the thickness of the plate for ν =0, 0.1, 0.2, 0.3, 0.4 and 0.45, respectively. Results of the same order of magnitude were obtained by Shivakumar and Raju [4].

3.4. Critical intersection angle

Bažant and Estenssoro [8] argued from energy and other considerations that the front edge of a propagating crack must terminate at the free surface obliquely, at a critical

angle which is a function of the Poisson's ratio, ensuring square-root singularity at the corner point. An analytical solution for the critical intersection angle is not available, although some numerical [2,3,9] solutions and experimental [1] data are available in the literature.
The critical intersection angle is calculated imposing square-root singularity at the corner point, for different Poisson's ratio values. The aim of the present work was not the calculation of the critical intersection angle, therefore results available in the literature were taken as a reference. Figure 7 presents data for β_c given in reference [16]. The solution given by the dashed curve was obtained by Heyder *et al.* [1] based on the 3D dual discontinuity method, the continuous line is an empirical equation proposed by Pook [10]. The solution proposed by Heyder *et al.* [16] was adopted in this work.

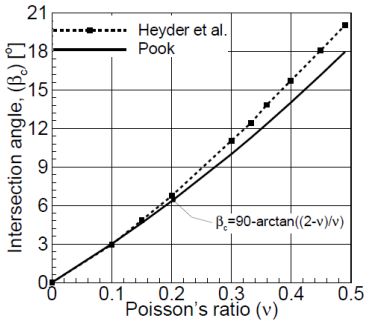

Figure 7. Intersection angle of the crack front with the free surface ensuring square-root singularity under mode I, after Heyder et al. [1].

3.5. Modification of the crack front geometry

As described above, the geometry of the crack front was modified (see Figure 8) in order to enforce square-root singularity at the corner point.

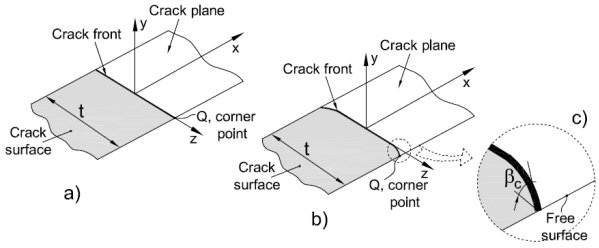

Figure 8. Different crack front geometries: a) Crack front normal to the free surface; b) and c)

The procedure adopted consisted of the following steps:
(1) Running a finite element simulation for a crack with a straight front, see Figure 8a;
(2) Calculation of the boundary layer thickness based on the log–log regression analysis previously described;
(3) Modifying the shape of the crack front in the boundary layer region so that for the chosen value of m the crack front intersects the free surface at the critical angle, see Figure 8b and c;
(4) Running a finite element analysis of the same problem with a modified crack front shape;
(5) Log–log regression analysis of the modified crack front problem and comparison of results.

Two different shapes were studied (see Figure 9): 1) a circular arc crack front within the boundary layer and 2) a linear crack front with a circular transition between the boundary layer and "plane strain" like region.

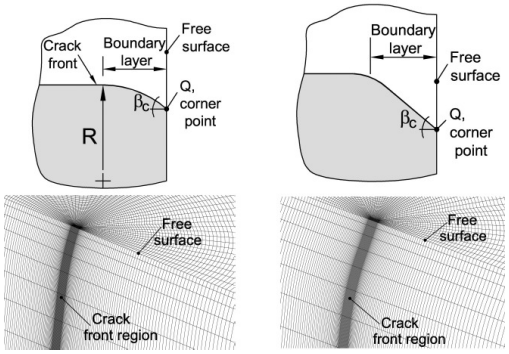

Figure 9. Geometrical and mesh details of different crack front shapes close to the free surface (ν=0.3).

Figure 8 and 9 show details of the modified crack front. Figure 10 shows the improvement in the power of the displacements obtained by modifying the shape of the crack front.

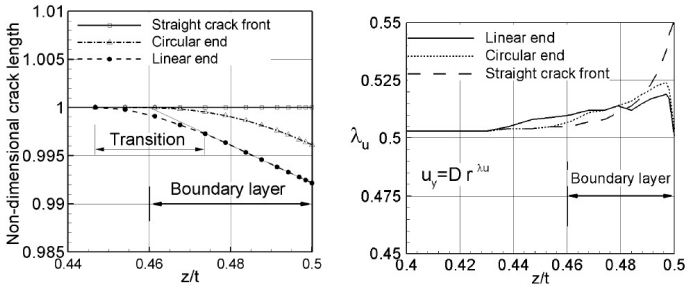

Figure 10. (a) Geometric details of the crack fronts close to the free surface; (b) power of the displacement for different crack front geometries and ν = 0.3.

It can be seen that within the boundary layer region a significant improvement takes place within 0.49 < z/t < 0.5, however little improvement is obtained for points further away from the free surface (0.44 < z/t < 0.49). The results obtained with both crack front geometries are quite similar, therefore for simplicity the crack front with the linear end close to the free surface was adopted for further calculations.

4. 3D FINITE ELEMENT MODELLING OF PLASTICITY-INDUCED CRACK CLOSURE

The aim of this section is to investigate the relevance of corner point singularities to the closure behaviour of 3D cracks. The first step is to characterize the closure behaviour of fatigue cracks with a crack front normal to the free surface for ν = 0, 0.2, 0.3 and 0.4. Secondly, for ν = 0.2, 0.3 and 0.4 the shape of the crack front will be modiffied according to the procedure previously described in order to assure a square-root singularity at the corner point.
Three-dimensional simulations of plasticity-induced crack closure were carried out using a standard node

release scheme [5]. The crack is allowed to grow by one element size by releasing nodes ahead of the initial crack front every two load cycles. The nodes are released sequentially by modifying the appropriate boundary conditions. The node displacement method was used to calculate the opening stresses. This method consists of monitoring the displacement of a node (the first node behind the crack tip in the present work) as the load is applied [11]. The opening stresses are found when the displacement of the node monitored became positive during the loading stage of a load cycle. It should be noted that issues such as mesh refinement, crack growth scheme, method of calculating the opening stresses and number of load cycles between node releases can affect the results. The current work does not seek to address any of these aspects explicitly, therefore all simulations were performed under the same conditions, i.e, same mesh density, crack growth scheme, opening stress calculation method and load conditions ($\sigma_{max}/\sigma_{yield}$ *=0.5 and R=0*).

Figures 11 a) and b) compare the opening stresses for the case of straight crack front a) and corrected crack front b) it can be seen that the different levels of stresses singularity along crack imposed by the elasticity solution do not seem to be of great practical significance in terms of the magnitude of the opening stress levels. For lower levels of remote applied stresses this difference may increase.

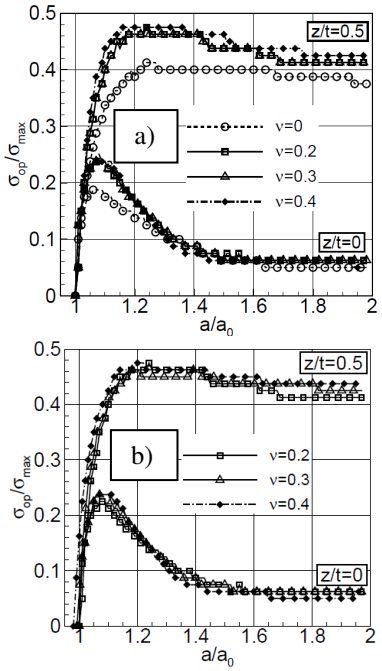

Figure 11. Comparison of the opening stresses for the case of straight crack front a) and corrected crack front b) respectively. $\sigma_{max}/\sigma_{yield}$ *=0.5, R=0 and* a_0*=1.0mm.*

5. DISCUSSION OF THE RESULTS AND CONCLUSIONS

The results presented show that modelling of plasticity-induced crack closure is not significantly influenced by the nature of the elasticity solution where the crack front meets the free surface. The effect of different types of stress singularities along the crack front for different values of the Poisson's ratio and crack front geometries was shown to have little effect on the closure behaviour in particular for $0.2 < \nu < 0.4$. It seems that, at least for the loading conditions used in the present work, the plasticity associated with the stress field along the crack front dominates the solution in such a way that the different levels of elastic stress singularity along the crack front do not have significant influence on the closure behaviour.

REFERENCES

[1] Heyder, M., Kolk, K., Kuhn, R.J., *Numerical and experimental investigations of the influence of corner singularities on 3D fatigue crack propagation*, International Journal of Fatigue, 72:2095-2105, 2006.

[2] Benthem, J.P., *State of Stress at Vertex of a Quarter-Infinite Crack in a Half-Space*, International Journal of Solids and Structures, 13(5):479-492, 1977.

[3] Benthem, J.P., *Quarter-Infinite Crack in a Half-Space - Alternative and Additional Solutions*, International Journal of Solids and Structures, 16(2):119-130, 1980.

[4] Shivakumar, K.N., Raju, I.S., *Treatment of Singularities in Cracked Bodies*, International Journal of Fracture, 45(3):159-178, 1990.

[5] de Matos, P.F.P., Nowell, D., *Numerical simulation of plasticity-induced fatigue crack closure with emphasis on the crack growth scheme: 2D and 3D analyses*, Engineering Fracture Mechanics, 75(8): 2087-2114, 2008.

[6] Roychowdhury, S., Dodds, R. H., *Three-dimensional effects on fatigue crack closure in small-scale yielding regine - a finite element study*, Fatigue & Fracture of Engineering Materials & Structures, 26:663-673, 2003.

[7] Dawicke, D.S., Grandt, A.F., *Three-Dimensional Crack Closure Behavior*. Engineering Fracture Mechanics, 36(1):111-121, 1990.

[8] Z. P. Bažant, Z.P., Estenssoro, L.F., *Surface Singularity and Crack-Propagation*, International Journal of Solids and Structures, 16(5):479-481, 1980.

[9] Hartranft, R.J., Sih, G.S., *An approximate three-dimensional theory of plates with application to crack problems,* International Journal of Engineering Science, 8:711-729, 1970.

[10] Pook, L.P., Some Implications of Corner Point Singularities, Engineering Fracture Mechanics, 48(3):367-378, 1994.

[11] de Matos, P.F.P., Nowell, D., *On the accurate assessment of crack opening and closing stresses in plasticity-induced crack closure problems*, Engineering Fracture Mechanics, 2007;74(10):1579–601.